Materials Science and Engineering C 58 (2016) 352–358

Contents lists available at ScienceDirect

Materials Science and Engineering C

journal homepage: www.elsevier.com/locate/msec

Probing the surface microstructure of layer-by-layer self-assembly chitosan/poly(L-glutamic acid) multilayers: A grazing-incidence small-angle X-ray scattering study

Nie Zhao, Chunming Yang *, Yuzhu Wang, Binyu Zhao, Fenggang Bian, Xiuhong Li, Jie Wang *

Shanghai Synchrotron Radiation Facility, Shanghai Institute of Applied Physics, Chinese Academy of Sciences, Shanghai 201204, People's Republic of China

ARTICLE INFO

Article history:
Received 27 February 2015
Received in revised form 18 August 2015
Accepted 25 August 2015
Available online 30 August 2015

Keywords:
Polyelectrolyte multilayer
Grazing-incidence
X-ray scattering
Resonant diffuse scattering

ABSTRACT

This study characterized the surface structure of layer-by-layer self-assembly chitosan/poly(L-glutamic acid) multilayers through grazing-incidence small-angle X-ray scattering (GISAXS), X-ray reflectivity (XRR), and atomic force microscopy (AFM). A weakly long-period ordered structure along the in-plane direction was firstly observed in the polyelectrolyte multilayer by the GISAXS technique. This structure can be attributed to the specific domains on the film surface. In the domain, nanodroplets that were formed by polyelectrolyte molecules were orderly arranged along the free surface of the films. This ordered structure gradually disappeared with the increasing bilayer number because of the complex merging behavior of nanodroplets into large islands. Furthermore, resonant diffuse scattering became evident in the GISAXS patterns as the number of bilayers in the polyelectrolyte multilayer was increased. Notably, the lateral cutoff length of resonant diffuse scattering for these polyelectrolyte films was comparable with the long-period value of the ordered nanodroplets in the polyelectrolyte multilayer. Therefore, the nanodroplets could be considered as a basic transmission unit for structure propagation from the inner interface to the film surface. It suggests that the surface structure with length scale larger than the size of nanodroplets was partially complicated from the interface structure near the substrate, but surface structure smaller than the cutoff length was mainly depended on the conformation of nanodroplets.

1. Introduction

Polyelectrolyte multilayers (PEMs) formed by the layer-by-layer technique [1,2] have attracted considerable interest because of their potential applications in optical devices [3–5], sensing [6–8], drug release [9,10], and biologically active coatings [11–15]. The PEM film is based on the alternating adsorption of oppositely charged polyions onto a charged surface. Their surface and internal structures [16–19] usually depend on complex deposition conditions, including chemical properties of solution (pH, ionic strength) [20], dielectric of substrate [21], and post-treatment method [22,23]. Therefore, the study of mechanisms that govern film growth and structuring during deposition becomes meaningful. In 2000, Ladam et al. [24] firstly proposed the zone model that the PEM film could be subdivided into three distinct zones. The first zone is comprised of several bilayers of polyelectrolytes close to the substrate. The conformation of polyelectrolyte molecules in this zone is mainly influenced by the nature of the substrate. The second zone forms the bulk of the PEM film and shows no evident stratified structures because of molecule diffusion and the influence of the substrate disappears, while the third zone is a highly free region close to the interface with the solution. During the past decade, several theoretical efforts as well as experimental works have been done to understand the growth of these three zones. Schlenoff [25] noted that the PEM film will form zone two when zones one and three have reached their final thickness. As more layers are added to the film, zones one and three are expected to keep their respective thickness and character and zone two will increase thickness.

To study the correlation between these three distinct zones, the roughness of the internal interface and film/air interface was characterized through X-ray and neutron reflectometry by Gopinadhan et al. [26]. Their results show that the film/air interface roughness almost coincides with the internal interface roughness as the deposition conditions were changed. It suggested that the roughness of both the internal interface and the film/air interface can be attributed to the same physical origin. Recently, Cornelsen et al. [27] proposed that the increase in surface roughness as a function of deposition steps is caused by spatially periodic structures (also called ordered structure) which are related to spinodal decomposition. The length scale of the periodic structure is on the order of several nanometers. According to our knowledge, however, the growth mechanism of these periodic structures has been rarely investigated. Furthermore, the roughness propagation effect between the internal interface and film/air surface has not been studied. Most of previous

* Corresponding authors.
E-mail addresses: yangchunming@sinap.ac.cn (C. Yang), wangjie@sinap.ac.cn (J. Wang).

http://dx.doi.org/10.1016/j.msec.2015.08.048
0928-4931/

studies principally relied on direct real-space observation methods, such as transmission or scanning electron microscopy. However, these methods are limited by their slow rate, sampling limits, artifacts, and restricted local probe. In addition, the internal interface structure could not be characterized by these traditional methods. By contrast, grazing-incidence small-angle X-ray scattering (GISAXS) [28] provides structural information averaged over macroscopic regions, is nondestructive, and can be used during preparation, post-treatments, or application.

Two polyelectrolytes selected for this study, chitosan (CS) and poly(L-glutamic acid) (PLGA), are both useful biological materials. Chitosan, a random copolymer constituted by N-glucosamine and N-acetylglucosamine units [29–31], is obtained by partial N-deacetylation of chitin, a natural constituent of different aquatic invertebrates. The degree of acetylation (DA) corresponds to the molar fraction of acetylated units within the polymer chains. CS is a very promising material in drug formulations [32], tissue engineering [33,34] and antibacterial treatments [35]. PLGA is a synthetic polymer where the naturally occurring L-glutamic acid was linked together through amide bonds. Since PLGA shows good hydrophilicity and biodegradability and is absent of antigenicity and immunogenicity [36,37], it becomes a promising material in drug delivery [14,38] and tissue engineering [39,40].

In the present study, GISAXS combined with XRR and AFM techniques was used to characterize the structure of the internal interface and film/air surface. A weakly long-period ordered structure along the in-plane direction was firstly observed in the chitosan (CS) and poly(L-glutamic acid) (PLGA) multilayer by the GISAXS technique. The periodic structures of PEMs were varied with the number of bilayers. Interestingly, resonant diffuse scattering was also observed in the GISAXS patterns of PEM films. The partial roughness propagation effect between the internal interface and the film/air interface was estimated. Our results provide insights into the microstructure and growth behavior of PEM films for biopolymers (i.e., polypeptides and polysaccharides).

2. Experimental section

2.1. Polyelectrolytes

Chitosan (448877-50G, DA: 75%–85%) and poly-L-glutamic acid sodium (P4761-100MG) were purchased from Sigma-Aldrich. Chitosan was successively dissolved at 1% (w/v) in a 0.1 M acetic acid solution. The concentration of chitosan solution was 0.2 mg/ml. The solution was adjusted to a fixed pH of 4.0 by adding 0.1 M NaOH. Poly-L-glutamic acid sodium was dissolved in ultrapure water with a concentration of 0.2 mg/ml. The pH of solution was also adjusted to 4.0 by adding 0.1 M acetic acid solution. The water used for all solutions and rinsing processes was ultrapure water (electrical resistivity $\rho > 18$ MΩ-cm) purified in a Milli-Q Academic purification stage (Millipore).

2.2. Multilayer build-up

One-side polished p-type (100) silicon substrates were purchased from the Kai Hua crystalline silicon material company (Zhejiang, China) and sectioned to 3 cm × 2 cm rectangles. The substrates were ultrasonically cleaned in a hot 98% H_2SO_4 and 27% H_2O_2 mixture with a 7:3 volume ratio and then extensively rinsed with ultrapure water. The substrates were dried by high-purity nitrogen before multilayer building processes. The cleaned substrates were dipped in a prepared polycation solution for 20 min, rinsed several times with ultrapure water, and then dried by nitrogen gas. The dried substrates were immersed in a polyanion solution for 20 min and then rinsed using the same procedure for upper deposition. Multilayers were obtained through repeated deposition of these two solutions. The samples were nitrogen-dried at the end of their fabrication.

2.3. Grazing incidence small angle X-ray scattering

GISAXS measurements were performed on the BL16B beam line ($E = 10$ keV) at the Shanghai Synchrotron Radiation Facility (SSRF, China). The samples were mounted on the sample stage, which can translate in three directions and rotate around two orthogonal axes. To control the penetration length, we chose an X-ray incident angle from 0.15° to 0.6°. The scattered intensity was collected as a function of the in-plane $2\theta_f$ and out-of-plane α_f angles on a 16-bit X-ray charge-coupled device (2048 × 2048 pixels, pixel size of 80 × 80 μm^2) placed at a distance of 1940 mm downstream from the sample. The direct incident beam and reflected beam were hidden by two beam stops before the detector. A schematic of the measurements is shown in Fig. 1.

2.4. X-ray reflectivity

XRR measurements of the PEM films with various bilayer numbers were performed on the D8 Advance. The incident beam (Cu Ka1 radiation, $\lambda = 1.54$ Å) was conditioned by a 2.5° soller slit, a 0.1 mm divergence slit, and a 0.1 mm Cu mask. The reflected X-ray intensity was collected by a LynxEye XE counter. Measurements were taken in θ–2θ mode geometry from 0.1° to 4.0° at a tube power of 40 kV/40 mA to maintain linearity in the detector response. XRR measurements were also performed at BL14B1 of the SSRF using a wavelength of 1.24 Å. The beam was focused by a Rh/Si mirror to the size of 0.5 mm × 0.5 mm. Data were obtained using an NaI point detector with a step size of 0.01°, scaled to unit incident intensity, and then corrected for spill over at low incoming angles (depending on sample size and divergence slit width). Film thickness and roughness were obtained through the XRR fitting software StochFit [41].

2.5. Atomic force microscopy imaging

The films were observed via AFM using a Multi-Mode Scanning Probe Microscope from Digital Instruments (Bruker AXS GmbH) with an "E" scanner, a NanoScope IIIA controller, and NanoScope version 5.31 software. "V"-shaped cantilevers with triangular silicon tips (NSC11, MikroMasch) with a nominal spring constant of 48 N/m were used to image the samples in tapping mode with a driving frequency of 356.8 kHz, a driving amplitude of 20 mV, and a scan rate of 1 Hz. During imaging, the set point was carefully tuned, and small values were used to protect the tips and samples. All AFM experiments were performed at ambient conditions.

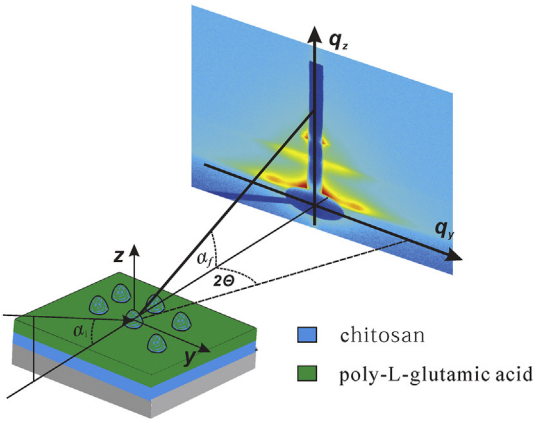

Fig. 1. Schematic of GISAXS in asymmetric reflection geometry, applied to a system of polyelectrolyte multilayer. The y_z plane was perpendicular to the incident beam direction. α_i, α_f, and $2\theta_f$ represent the angle incident beam with respect to the sample surface, the scattered beam with respect to the sample surface, and the in-plane angle with respect to the transmitted beam, respectively.